Polymer 51 (2010) 694–701

Contents lists available at ScienceDirect

Polymer

journal homepage: www.elsevier.com/locate/polymer

Hyperbranched fluorinated polyimides with tunable refractive indices for optical waveguide applications

Hong Gao, Changqing Yan, Shaowei Guan, Zhenhua Jiang*

Alan G. MacDiarmid Institute, Jilin University, Changchun 130012, P. R. China

ARTICLE INFO

Article history:
Received 27 February 2009
Received in revised form
29 September 2009
Accepted 5 October 2009
Available online 21 October 2009

Keywords:
Hyperbranched polyimide
Tunable refractive indices
Optical waveguide

ABSTRACT

A series of halogenated hyperbranched polyimides (HBPIs) with tunable refractive indices (RIs) has been designed and prepared for use as novel optical waveguide materials. The hyperbranched structure of these polymers leads to multifarious and controllable chemical structures. The degree of branching in these HBPIs was estimated using ^{1}H NMR spectroscopy. The halogen-terminated HBPIs were found to exhibit high glass transition temperature, good thermal stability, excellent transparency, low birefringence and low optical loss in the wavelength windows for telecommunication. Due to the high polarizability of the C–Cl bond at the terminal groups, RIs were precisely controlled by adjusting the C–Cl bond content without additional optical losses. Finally, several waveguide devices were fabricated by the reactive ion etching (RIE) technique and were found to exhibit good optical propagation at a wavelength of 1.55 μm.

1. Introduction

Polymer optical waveguides have attracted considerable attentions for their possible application as light transmission components in optical communication systems [1–3]. For advanced integrated optical waveguide applications such as optical attenuators, optical interconnects, splitters and arrayed waveguide gratings (AWG), the polymer optical materials should have excellent properties in terms of low optical losses, low birefringence [4,5], and high T_g. Waveguides devices with complex structures are often expected to meet more severe requirements, such as control of RIs, good interfacial adhesion, and similar coefficients of thermal expansion (CTE) [6].

In order to satisfy these requirements, various types of optical polymers have been arranged and developed. Among these polymers, the fluorinated polyimides are a class of promising waveguide materials due to their high thermal stability, high optical transparency and low optical losses at the wavelength windows for telecommunication (the central wavelengths are 0.85, 1.31, and 1.55 μm).[7–9] In case of linear fluorinated polyimides (LFPIs), copolymerization has been employed to control RIs, as demonstrated in the 6FDA/PMDA-TFDB copolymer system whose RIs are controllable over a wide range by varying the 6FDA content [10,11]. Although RIs of polyimides increase with increasing content of non-fluorinated dianhydride, a higher content of non-fluorinated dianhydride is undesirable because it often leads to higher optical loss with the increment of C–H bonds. In addition, LFPIs deposited on a silicon or silica substrate usually exhibit a large in-plane/out-of-plane birefringence, a result of both chain orientation on the film plane and the residual stress in the polyimide films originated from the CTE mismatch between the films and substrates [12]. Current efforts to develop optical waveguide polyimides are aimed at the design and synthesis of novel fluorinated polyimides with excellent optical properties. Hyperbranched structures have played an increasingly important role in reducing the birefringence [13,14] and allow facilitated tailoring of RIs [15].

In recent years, the hyperbranched polyimides (HBPIs) have been widely examined in many potential applications, such as gas separation and photo-patterning. Fang et al. first reported the preparation of HBPIs which were derived from a triamine (tris(4-aminophenyl)-amine) and several dianhydrides, and investigated their physical and gas transport properties as well [16,17]. Yin et al. synthesized another triamine (1,3,5-tris(4-aminophenoxy) benzene) for the preparation of HBPIs [18]. However, these monomers without fluorine do not fit for the application of HBPI as optical waveguide materials due to the high C–H content and low optical transparency. In our previous work, a fluorinated triamine (1,3,5-Tris(2-trifluoromethyl-4-aminophenoxy)benzene) was synthesized and polymerized into the HBPIs, and it was considered as a promising candidate for optical waveguide materials [19].

* Corresponding author. Tel./fax: +86 431 85168886.
E-mail address: jiangzhenhua@jlu.edu.cn (Z. Jiang).

0032-3861/$ – see front matter © 2009 Published by Elsevier Ltd.
doi:10.1016/j.polymer.2009.10.005

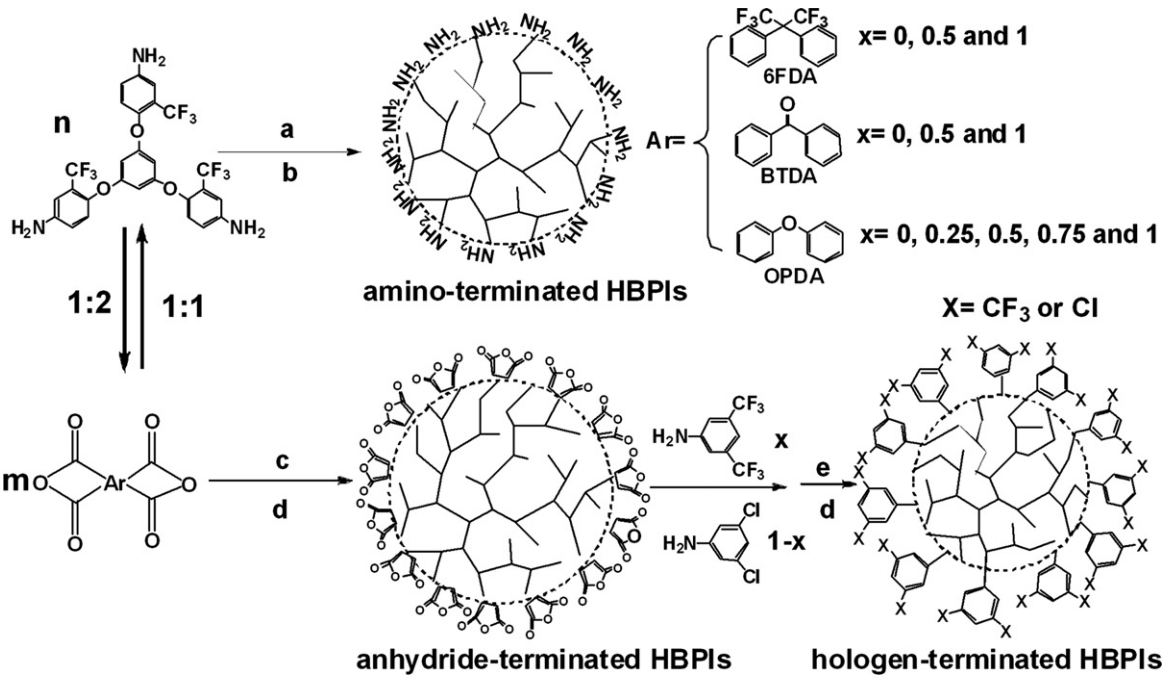

Scheme 1. Synthesis of HBPIs: (a) $m/n = 1{:}1$, a dianhydride solution was added to a TFAPOB solution, 40 °C, 24 h, (b) chemical imidization, *m*-xylene 170 °C, 5 h; (c) $m/n = 2{:}1$, a TFAPOB solution added to a dianhydride solution, 40 °C, 24 h, (d) chemical imidization, triethylamine, acetic anhydride, 40 °C, 8 h; (e) 3,5-ditrifuoromethylaniline ($2CF_3$) and 3,5-dichloroaniline (2Cl) with different ratio added to the solution of anhydride-terminated PAA, 40 °C for 8 h.

In this paper, a series of HBPIs with different halogenated terminal groups were prepared and characterized as novel optical waveguide materials, and their physical and optical properties of HBPI were examined. By copolymerizing HBPIs with different halogen-containing terminal groups, the RIs were precisely controlled without additional optical loss. These HBPIs with similar chemical structures were promising candidates for both the core and cladding of waveguides. Furthermore, several waveguide devices were fabricated from the HBPIs by the RIE technique, and their optical properties were investigated.

2. Experimental section

2.1. Materials

The synthesis of 1,3,5-Tris(2-trifluoromethyl-4-aminophenoxy)benzene (TFAPOB) had been reported elsewhere [19]. 4,4′-(Hexafluoroisopropylidene)diphthalic anhydride (6FDA), 4,4′-Oxydiphthalic anhydride (ODPA) and 3,3′-4,4′-Benzophenonetetracarboxylic dianhydride (BTDA) were purified by recrystallization from acetic anhydride before use. 3,5-bis(trifluoromethyl)aniline and 3,5-Dichloroaniline were purchased from Aldrich Chemical Co. and used without further purification. *N*,*N*-dimethylacetamide (DMAc) was refluxed in presence of CaH_2 and distilled under vacuum before use.

2.2. Characterization

Differential scanning calorimetry (DSC) was performed on a Mettler Toledo DSC821^e at a heating rate of 20 °C/min under a nitrogen atmosphere. The thermogravimetric analysis (TGA) was performed using a Perkin Elmer TGA-7 thermal analyzer system at the heating rate of 10 °C/min under a nitrogen atmosphere. Fourier transformed

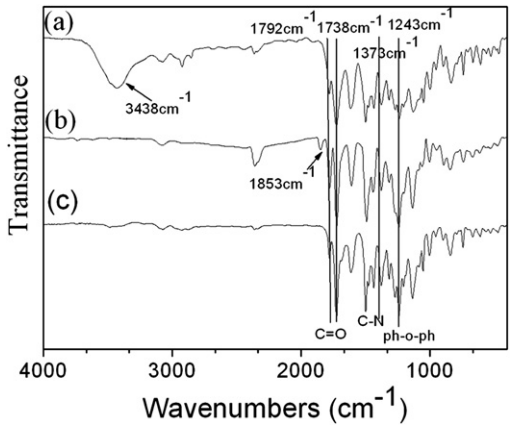

Fig. 1. IR spectra of ODPA-based HBPIs: (a) amino-terminated AM-OD, (b) anhydride-terminated AD-OD, (c) halogen-terminated HG-OD ($2CF_3$100%).

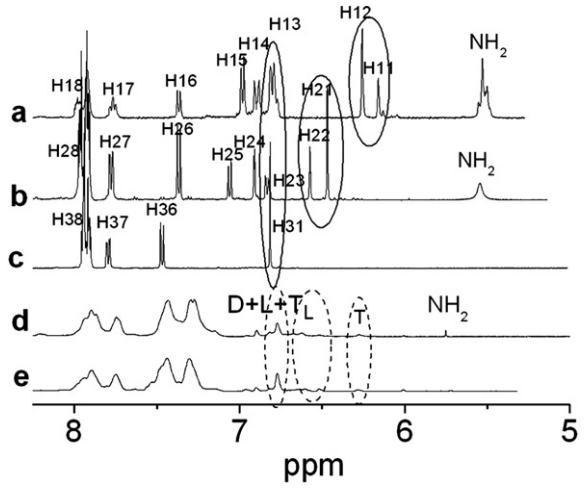

Fig. 2. ^{1}H NMR spectra of model compounds and 6FDA-based HBPI, (a) model 1, (b) model 2, (c) model 3, (d) AM-6F, and (e) AD-6F.

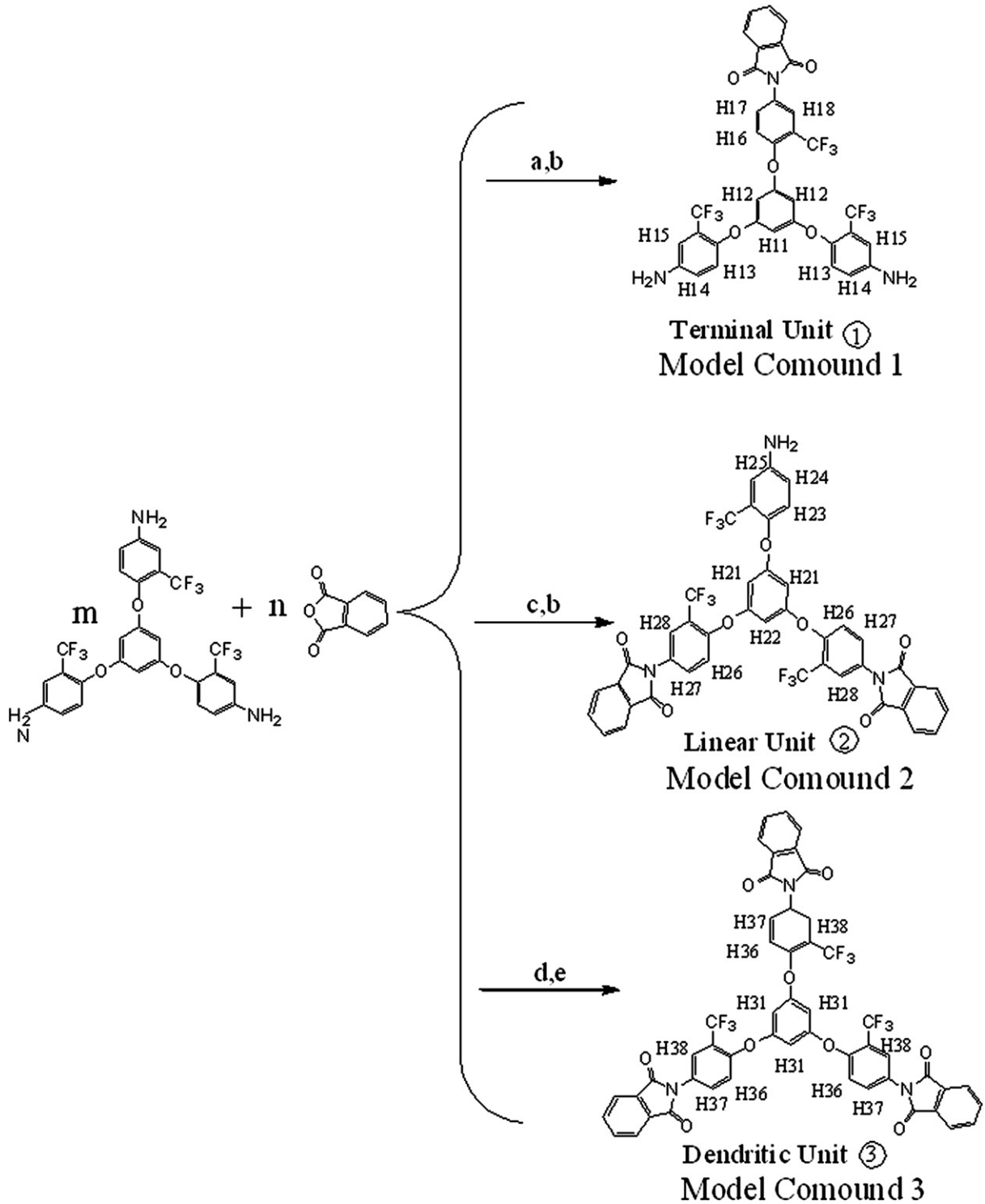

Scheme 2. Synthesis of the model compounds: (a) $m/n = 1/1$, 40 °C, 5 h; (b) chemical imidization, *m*-xylene, 170 °C, 5 h; (c) $m/n = 1/2$, 40 °C, 5 h; (d) $m/n = 1/3$, 40 °C, 12 h; and (e) chemical imidization, triethylamine, acetic anhydride, 40 °C, 12 h.

FT-IR spectra (KBr) were measured using a Nicolet Impact 410 infrared spectrometer. Gel permeation chromatograms (GPC) were obtained by a Waters 410 instrument with tetrahydrofuran (THF) as the eluent and polystyrene as the standard. The ^{1}H and ^{19}F NMR spectra were recorded at 500 and 470.5 MHz using a Bruker 510 NMR spectrometer with tetramethylsilane and $CFCl_3$ as the references (0 ppm) respectively. Near-infrared spectra (Near-IR) were measured on a Varian Kera 500 spectrometer. RIs of polymer films were measured by a J.A. Woollam M-2000UI spectroscopic ellipsometer. In-plane/out-of-plane birefringences (at 650 nm) of the polymer films was determined from the coupling angles of TE (transverse electric) or TM (transverse magnetic) optical guided modes with a gadolinium gallium garnet (GGG) prism at 650 nm. UV–visible absorption spectra were recorded on a UV2501-PC spectrophotometer. Scanning electron micrographs (SEM) were observed on a SHIMADZU SSX-550 microscope. Atomic force microscopy (AFM) of film surfaces were

Table 1
Physical properties of the HBPIs.

Polymers	x(mol%)[a]	M_n[b]	M_w/M_n	T_g(°C)[c]	T_d(°C)[d]	DB[e]
AD-OD	–	13,000	2.17	220	516	0.93
AM-OD	–	27,000	1.96	240	528	0.60
HG-OD (2CF_3 100%)	1	19,000	2.02	217	530	
HG-OD (2CF_3 50%)	0.5	27,000	3.05	212	526	
HG-OD (2CF_3 0%)	0	25,000	2.71	202	502	
AD-BT	–	10,000	1.96	230	526	0.90
AM-BT	–	15,000	2.50	241	532	0.66
HG-BT (2CF_3 100%)	1	22,000	2.07	242	515	
HG-BT (2CF_3 50%)	0.5	15,000	2.24	227	512	
HG-BT (2CF_3 0%)	0	26,000	2.55	220	508	
AD-6F [19]	–	6, 000	1.92	232	506	0.87
AM-6F [19]	–	26,000	1.96	243	523	0.62
HG-6F[19] (2CF_3 100%)	1	16,000	2.55	242	514	
HG-6F (2CF_3 50%)	0.5	33,000	2.24	234	515	
HG-6F (2CF_3 0%)	0	28,000	3.52	226	526	

[a] Molar ration of (3,5-di-trifluoromethyl)aniline to the total terminated group.
[b] Number average molecular weight determined by GPC in THF vs polystyrene.
[c] Glass transition temperature measured by DSC with a heating rate of 10 °C/min in nitrogen.
[d] Onset temperature for 5% weight loss measured by TGA with a heating rate of 10 °C/min in nitrogen.
[e] Determined by ^{1}H NMR analysis.

observed with a Digital Instrument, Nanoscope IIIa. AFM tapping mode images were taken at room temperature in air with the microfabricated rectangle crystal silicon cantilevers (Nanosensor). Topographic images were obtained at a resonance frequency of ca. 365 kHz for the probe oscillation.

2.3. Prepareation of model compounds

2.3.1. Synthesis of model compound ***1***

TFAPOB (0.302 g, 0.5 mmol) was dissolved in 10 mL of DMAc in an oven dried, three-necked flask with stirring under a nitrogen atmosphere. A solution of 0.074 g (0.5 mmol) of phthalic anhydride in 5 mL of DMAc was added dropwise through a syringe over 0.5 h. After the addition, the reaction was further conducted for 5 h at 40 °C. Then, 30 mL of *m*-xylene was added, and the mixture was heated to 170 °C with a Dean–Stark apparatus for 5 h. After cooling to room temperature, the solution was precipitated from ice water. The crude product was dried *in vacuo* and purified by column chromatography with silica gel and a mixture of ethanol/cyclohexane (1/1, by volume) as the eluant to give a yellow powder.

EIMS *m*/*e*: 733. ^{1}H NMR (500 MHz, DMSO-d_6, ppm) δ: 8.02 (1H), 7.95–7.86 (4H, Ar–H of phthalic anhydride residues), 7.76 (1H), 7.37 (1H), 6.98 (2H), 6.90 (2H), 6.79 (2H), 6.24 (2H), 6.15 (1H), 5.51 (4H, NH_2).

2.3.2. Synthesis of model compound ***2***

The aforementioned procedure for the synthesis of model compound **1** was followed except that 0.148 g (1 mmol) of phthalic anhydride was used, then the final reaction solution was poured into ice water. The crude product was dried *in vacuo* and was also purified by column chromatography, a mixture of ethanol/cyclohexane (1/2) was used as the eluant.

EIMS *m*/*e*: 863. ^{1}H NMR (500 MHz, DMSO-d_6, ppm) δ: 8.02 (2H), 7.97–7.85 (8H, Ar–H of phthalic anhydride residues), 7.78 (2H), 7.36 (2H), 7.05 (1H), 6.91 (1H), 6.82 (1H), 6.56 (1H), 6.46 (2H), 5.55 (2H, NH_2).

2.3.3. Synthesis of model compound ***3***

A mixture of 0.302 g (0.5 mmol) of TFAPOB, 0.222 g (1.5 mmol) of phthalic anhydride, and 10 mL of DMAc was magnetically stirred under a nitrogen flow in a oven dried 100-mL, three-necked flask at 40 °C for 12 h. Subsequently, a mixture of 1 g of triethylamine and 3 g of acetic anhydride was added. The solution was kept at 40 °C for 12 h and then condensed under reduced pressure to give a yellow precipitate. The crude product was collected by filtration and recrystallized with *N*-methylpyrrolidinone (NMP).

EIMS *m*/*e*: 993. ^{1}H NMR (500 MHz, DMSO-d_6, ppm) δ: 8.02 (3H), 7.97–7.87 (12H, Ar–H of phthalic anhydride residues), 7.79 (3H), 7.37 (3H), 6.81 (3H).

2.4. Polymer synthesis

2.4.1. Synthesis of amino-terminated HBPIs

The general polymerization method for amino-terminated HBPIs was reported elsewhere [13]. A typical procedure for the polyaddition of TFAPOB with ODPA is described as follows. TFAPOB (0.604 g, 1 mmol) was dissolved in DMAc (10 cc) in a oven dried, three-necked flask under a nitrogen flow. A solution of ODPA dianhydride (0.302 g, 1 mmol) in DMAc (10 cc) was added dropwise to the mixture through a syringe over 1 h under magnetic stirring at 40 °C. The reaction was further conducted for 24 h. Then, *m*-xylene (10 cc) was added, and the reaction mixture was heated to 170 °C for 5 h with a Dean–Stark trap. After cooling to room temperature, the mixture was precipitated from ethanol (200 cc). The polymers were collected by filtration and dried under vacuum at 80 °C for 24 h. In this study, the amino-terminated HBPIs obtained from ODPA, BTDA and 6FDA dianhydrides will be referred to as AM-OD, AM-BT and AM-6F, respectively.

2.4.2. Synthesis of anhydride-terminated HBPIs

The general polymerization procedure is outlined in Scheme 1. A typical procedure for the polyaddition of TFAPOB with ODPA is introduced as follows. To a solution of 2 mmol (0.62 g) dianhydrde (ODPA) in dried DMAc (10 cc) in a 50 mL flask, 1 mmol (0.604 g) of TFAPOB dissolved in 5 mL of DMAc was added dropwise through a syringe over 1 h. The mixture was stirred at 40 °C for 24 h to afford anhydride-terminated poly(amic acid) (PAA) solution. The PAA was subsequently converted to PI through a chemical imidization process. The chemical imidization was carried out via the addition of 1 g of triethylamine and 3 g of acetic anhydride into the PAA solution at 40 °C for 8 h. The resulting homogeneous PI

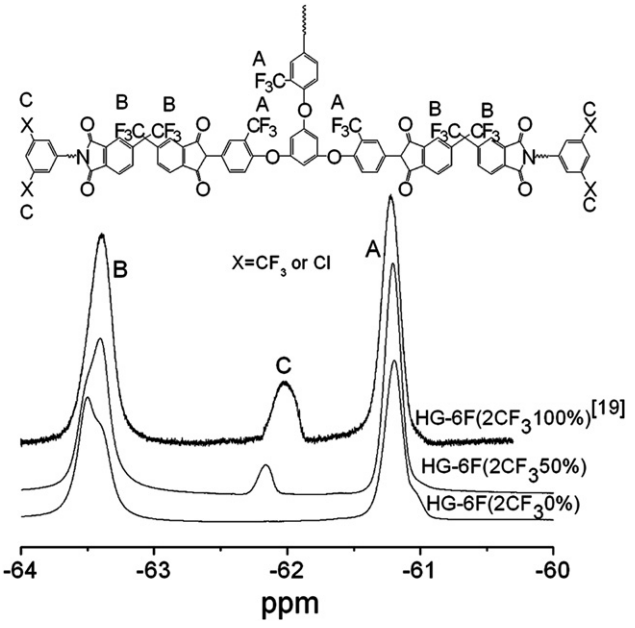

Fig. 3. ^{19}F NMR spectra of the HG-6F series.

Table 2
Solubility of the HBPIs.

Polymers	Solvents[a]						
	NMP	DMAc	DMSO	THF	$CHCl_3$	Actone	Ethanol
AD-OD/AM-OD	++	++	++	+	–	–	–
HG-OD series	++	++	++[b]	++	+[b]	–	–
AD-BT/AM-BT	++	++	++	+	–	–	–
HG-BT series	++	++	+[b]	++	–[b]	–	–
AD–6F/AM-6F[19]	++	++	++	+	+	–	–
HG-6F series	++	++	++	++	+	–	–

Qualitative solubility was determined with as 10 mg of polymer in 1 mL of solvent. ++: soluble at room temperature; +: soluble on heating at 100 °C; – insoluble.
[a] NMP, *N*-methyl-2-pyrrolidone; DMAc, *N*,*N*-dimethylacetamide; DMSO, dimethyl sulfoxide; THF, tetrahydrofuran.
[b] Special samples: The solubility of HG-OD($2CF_3$0%) and HG-BT($2CF_3$0%) were "+" in DMSO and is "–" in $CHCl_3$.

solution was poured into ethanol to give a white precipitate, which was collected by filtration, washed thoroughly with ethanol and dried under vacuum at 80 °C for 24 h. The anhydride-terminated HBPIs obtained from ODPA, BTDA and 6FDA will be referred to as AD-OD, AD-BT and AD-6F, respectively.

2.4.3. Synthesis of halogen-terminated HBPIs

The 3,5-bis(trifuoromethyl)aniline (x mmol) ($x = 0$, 0.5, 1) and 3,5-dichloroaniline (1-x) were both added into an equimolar amount of PAA precursors for AD-OD that was prepared by the same procedures. The reaction mixtures were stirred at 40 °C for 8 h. Then, a mixture of triethylamine (1 g) and acetic anhydride (3 g) was added, and was stirred at 40 °C for another 8 h. After cooling to room temperature, the mixture was precipitated from ethanol (200 cc). The polymers were collected by filtration and dried under vacuum at 80 °C for 24 h. The halogen-terminated HBPIs obtained from ODPA were signed as HG-OD ($2CF_3$ 100%) ($x = 1$), HG-OD ($2CF_3$ 50%) ($x = 0.5$), and HG-OD ($2CF_3$ 0%) ($x = 0$). HG-BT and HG-6F series were also prepared using the same procedure. The polymer of $x = 0.25$ and 0.75 were prepared for the series of HG-OD to estimate the controllability of refractive index. The polymerization procedures were also outlined in Scheme 1.

2.5. Film preparation for optical measurement

The HBPIs thus synthesized were dissolved in cyclohexanone at a concentration of 10 wt%. The solution was filtered with a 1 μm Teflon membrane syringe filter. The filtered solution was spin-coated onto a silicon wafer and fused silica substrate at a spin rate of 1500 rpm for 1 min. followed by curing at 140 °C for 4 h, 200 °C for 1 h and 250 °C for 1 h. By adjusting the concentration of PI solutions, the film thickness was controlled in the range of 2–4 μm.

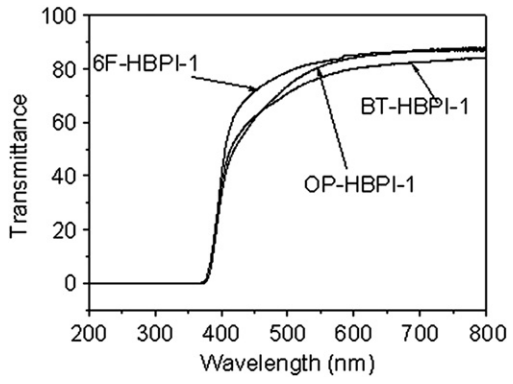

Fig. 4. UV-vis spectra of the halogen-terminated HBPIs.

2.6. Waveguide fabrication

Three layered rib-type optical waveguides were fabricated by spin coating PI solution for the under-cladding and core onto an fues silicon substrate. Next, the aluminum layer was sputtered onto the core layer and patterned by photolithography. Then a core waveguide was produced using oxygen RIE. After that, the mask was removed and the core ridges were formed. Finally, the core ridges were covered with PMMA layer with lower refractive index.

3. Results and discussion

3.1. Polymer synthesis

HBPIs were first prepared from $A_2 + B_3$-type monomers by Fang [16]. In this work, the same method was employed to synthesize a series of halogen-terminated HBPIs for the fabrication of waveguide devices. The three-step synthetic procedure is shown in Scheme 1. Three dianhydrides (6FDA, ODPA, BTDA) and triamine (TFAPOB) were condensed with different monomer addition orders and molar ratios to form different hyperbranched PAA precursors. Subsequently, the halogen-terminated monomers (3,5-bis(trifuoromethyl)aniline and 3,5-dichloroaniline) were added into the anhydride-terminated precursors for end-capping, then all the PAAs precursors were chemically imidized to give the corresponding HBPIs. The structures of the amino-, anhydride-, and halogen-terminated HBPIs were confirmed by FT-IR and ^{1}H NMR spectroscopy. Fig. 1 shows the IR spectra of AM-OD, AD-OD and HG-OD ($2CF_3$, 100%) HBPIs. The absorption peaks at 1792 cm^{-1} (C=O asymmetrical stretching), 1738 cm^{-1} (C=O symmetrical stretching) and 1373 cm^{-1} (C–N stretching) are the characteristic absorption bands for PI, and no characteristic band of PAA (1680 cm^{-1}) is detected. As for the amino-terminated HBPI (a), the band at 3438 cm^{-1} is assigned to the stretching absorption of N–H at the terminal amino groups. The peak at 1853 cm^{-1} (C=O stretching) indicates the existence of terminal anhydride groups for the anhydride-terminated HBPIs (b), while, No such two absorption bands are found in the halogen-terminated HBPIs (c), and this phenomenon demonstrates that halogen-termination was successfully achieved.

The structural perfection of hyperbranched polymers has been generally characterized by the degree of branching (DB), which was defined by Frechet as follows:[20]

$$DB = (D + T)/(D + T + L) \quad (1)$$

where *D*, *T*, and *L* refer to the numbers of dendritic, terminal, and linear units in the polymer, respectively. Experimentally, DB is usually estimated from ^{1}H NMR or ^{13}C NMR spectroscopy by comparing the integrals of peaks assignable to respective units. Fig. 2 shows ^{1}H NMR spectra of the amino-terminated and anhydride-terminated HBPIs derived from 6FDA. For the amino-terminated AM-6F, the peaks in the range of 8.16–7.75 ppm are assignable to the hydrogens of 6FDA residues, while the peaks in the range 7.56–6.18 ppm were corresponds to the hydrogens in the phenyl rings of TFAPOB residue, which contain the information on the degree of branching. The peak at 5.48 ppm is attributable to the free amino hydrogens in the terminal and linear units. To clarify the detailed assignment of peaks in the range of 7.56–6.18 ppm, three kinds of model compounds were synthesized from phthalic anhydride and TFAPOB as shown in Scheme 2. The TFAPOB residues in model compounds **1**, **2**, and **3** are basically same as the counterparts

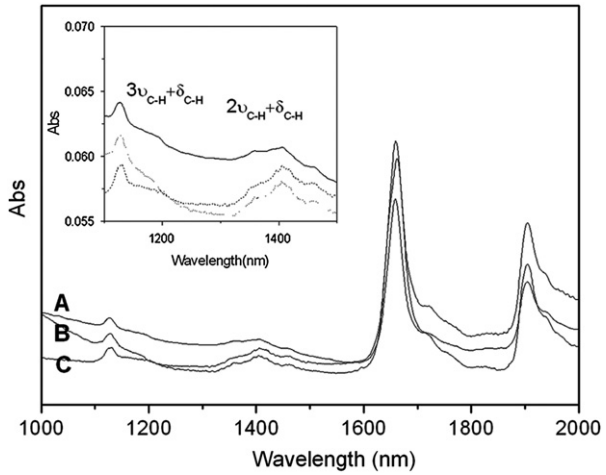

Fig. 5. Near-IR spectra of HG-OD (A: HG-OD ($2CF_3$ 100%); B: HG-OD ($2CF_3$ 50%), and C: HG-OD ($2CF_3$ 0%)).

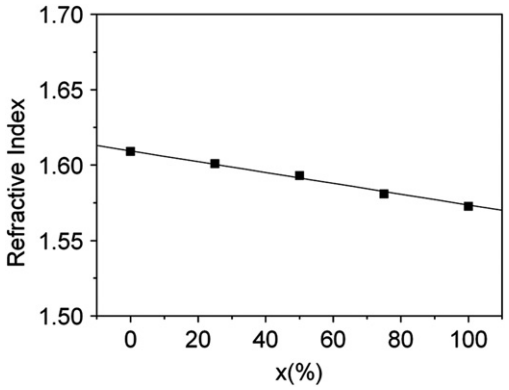

Fig. 6. Relationship between the RIs and the content of 3,5-bis(trifluoromethyl)aniline (x = molar ratio of 3,5-bis(trifluoromethyl)aniline to the total terminal groups).

in terminal, linear, and dendritic units of the HBPI, respectively. For comparison, their ^{1}H NMR spectra are also shown in Fig. 2(a–c). The peaks in the range of 7.56–6.18 ppm observed for the amino-terminated AM-6F can be compared with those of model compounds 1, 2 and 3 as well as that for anhydride-terminated AD-6F. Model 1 demonstrates eight distinct peaks at 8.02 (H18), 7.76 (H17), 7.37 (H16), 6.98 (H15), 6.90 (H14), 6.79 (H13), 6.24 (H12) and 6.15 ppm (H11). Model 2 also exhibits eight distinct peaks but with different chemical shifts at 8.02 (H28), 7.78 (H27), 7.36 (H26), 7.05 (H25), 6.91 (H24), 6.82 (H23), 6.56 (H22) and 6.46 ppm (H21). Model 3 exhibits four distinct peaks at 8.02 (H38), 7.79 (H37), 7.47 (H36), 6.81 (H31). The amino-terminated AM-6F demonstrates the peaks in the range of 7.62–7.78 ppm which includes the overlapping signals from the terminal H17, linear H27, and dendritic H37. In addition, the peaks in 7.20–7.50 ppm include the overlapping signals from the terminal H16, linear proton H26, and dendritic proton H36. The peak around 6.78 ppm is related to both the terminal H14, H15 and the linear H24, H25. Furthermore, the peak at 6.73 ppm corresponds to the terminal H13, linear H23, and dendritic H31. Therefore, the margin of the integration of latter two peaks can afford the resonance of dendritic proton H31. The peaks around 6.52 ppm are assignable only to the linear H21 and H22, while the peak at 6.14 ppm is independently ascribed to the terminal H11 and H12. The integral of the terminal units is very close to that of the dendritic units, which indicates that the DB of the amino-terminated HBPI was estimated as 62% according to eq. (1). The ^{1}H NMR spectra of AM-OD and AM-BT display peaks with the chemical shifts similar to those of AM-6F, and the DB values were calculated as 60% and 66%, respectively. The DB values higher than 0.5, which are for a statistic growth [21], could be caused by the low conversion of the amino groups. As shown in Table 1, the DB values for the amino-terminated HBPIs are dependent on their molecular weights. A lower molecular weight means lower conversions of the amino groups, which correspond to a higher DB values.

For the anhydride-terminated AD-6F, supposing the amino groups of TFAPOB monomer are reacted (i.e., TFAPOB residues are completely "dendritic"), the HBPI should have the "completely branched" structure (DB = 1). However, it should be noted that the anhydride-terminated HBPIs are less perfect in structure than common dendrimers due to the random polymerization process. In Fig. 2(e), a resonance in 6.2–6.4 ppm is detectable, which indicates that the polymers also have linear and terminal units, and the estimated DB value is 87%. The same phenomena were also observed in the NMR spectra of anhydride-terminated AD-OD and AD-BT, in which the estimated BD values were 93% and 90%, respectively. As for the anhydride-terminated HBPIs, large amount of semidendritic units may exist, however, the estimated DB values could be still higher than the actual values; for halogen-terminated HBPIs, the amino groups of the linear units are capped by the end groups, and so the linear and terminal units are not detectable in the NMR analysis. Therefore, the DB value is not sufficiently effective to express the structural perfection of HBPI in this case.

In the case of halogen-terminated HBPIs, ^{1}H NMR spectra are unable to confirm the structure of the terminal halogen groups in detail, and different halogen-terminated structures are characterized by ^{19}F NMR (Fig. 3). The peaks observed at −61.5 ppm and −63.7 ppm are attributable to the $-CF_3$ groups of 6FDA and triamine, respectively and the peak at −62 ppm is assignable to the $-CF_3$ associated with the terminal monomer of 3,5-ditrifuoromethylaniline. No fluorine signal relating to the 3,5-dichloroaniline-terminated HBPIs was detected. It is notable that the fluorine contents in the HBPIs can be easily controlled by varying the feed ratio of the terminal monomer. This property is advantageous for the resulting HBPIs in waveguide applications because the facile structural control and reproducibility of optical properties such as refractive index are critical for the design and fabrication of waveguide devices.

Table 1 illustrates the physical properties of the HBPIs. The molecular weights (M_n) and the polydispersities were estimated as 6,000–33,000 and 1.92–3.52, respectively. All the HBPIs exhibit good thermal properties with the 5% weight loss at temperatures above 500 °C. The DSC thermograms revealed the glass transition

Table 3
Optical properties of the halogen-terminated HBPIs.

Polymers	Refractive index[a]		Birefringence[b]		
	1.31 μm	1.55 μm	Refractive index at 650 nm		$n_{TE}-n_{TM}$
			TE mode (n_{xy})	TM mode (n_z)	
HG-OD ($2CF_3$ 100%)	1.5807	1.5727	1.6252	1.6154	0.0098
HG-OD ($2CF_3$ 50%)	1.5970	1.5930	1.6293	1.6199	0.0094
HG-OD ($2CF_3$ 0%)	1.6109	1.6090	1.6326	1.6253	0.0073
HG-BT ($2CF_3$ 100%)	1.5863	1.5842	1.6362	1.6247	0.0086
HG-BT ($2CF_3$ 50%)	1.5883	1.5846	1.6381	1.6325	0.0056
HG-BT ($2CF_3$ 0%)	1.5944	1.5851	1.6360	1.6330	0.0060
HG-6F [19] ($2CF_3$ 100%)	1.5160	1.5140	1.5542	1.5521	0.0021
HG-6F ($2CF_3$ 50%)	1.5234	1.5206	1.5564	1.5538	0.0026
HG-6F ($2CF_3$ 0%)	1.5309	1.5254	1.5585	1.5542	0.0043

[a] The refractive indices of the polymer films were obtained using a spectroscopic ellipsometer.
[b] The birefringence of the polymer films were measured by the method of coupling angles of TE or TM optical modes with a prism at 650 nm.

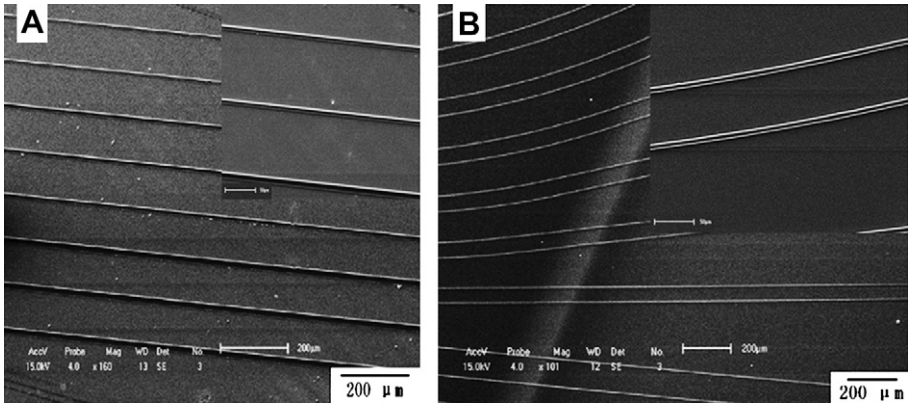

Fig. 7. SEM micrographs of the waveguide devices: straight waveguide (A) and flexural waveguide (B).

temperatures (T_g) of the HBPIs ranged from 200 to 243 °C. T_g's of the halogen-terminated HBPIs are lowered due to the chemical substitution at the terminal group, which can be explained by the reduction in the end group polarity of the amino- and anhydride-terminated HBPIs. All the HBPIs display excellent solubilities in common organic solvents, such as DMAc, NMP and cyclohexanone (Table 2). The solubility of the halogen-terminated HBPIs is better than that of the anhydride-terminated HBPIs, which is attributed to the enhanced polarity of the terminal groups [22]. All the HBPIs readily form tough, flexible, and optically transparent films by casting or spin coating techniques, properties essential in optical applications.

3.2. Optical properties

As shown in Fig. 4, the UV-vis spectra of the HG-6F series exhibit cut-off wavelengths around 370 nm and the transparency is around 85% in the range of 380–800 nm. This excellent optical transparency of the fluorinated HG-6F is attributed to the reduced formation of intermolecular charge-transfer-complexes (CTC) between the electron-donating triamine and the electron-acceptor dianhydride. Bulky, electron-withdrawing $-CF_3$ groups attached to the polymer backbones may induce this effect. On the other hand, it has been assumed that the intermolecular packing in hyperbranched polymer chains is incompact, which prevents CTC formation and may enhance the optical transparency in the visible region.

Low optical loss in the near-IR region is one of the most important requirements for waveguide materials. In our previous paper, we have reported that the end-capping by $-CF_3$ is an effective route to improve the optical transparency of HBPIs in the near-IR region for telecommunication region [19]. In this study, the absorptions in the halogen-terminated HBPIs were also researched by near-IR absorption spectra Fig. 5. Absorption peaks are normalized by dividing with their film thickness. The first combination bands $2\nu + \delta$ and the weak combination bands $3\nu + \delta$ of the C–H stretching and bending, appear in the region of 1.25–1.4 μm

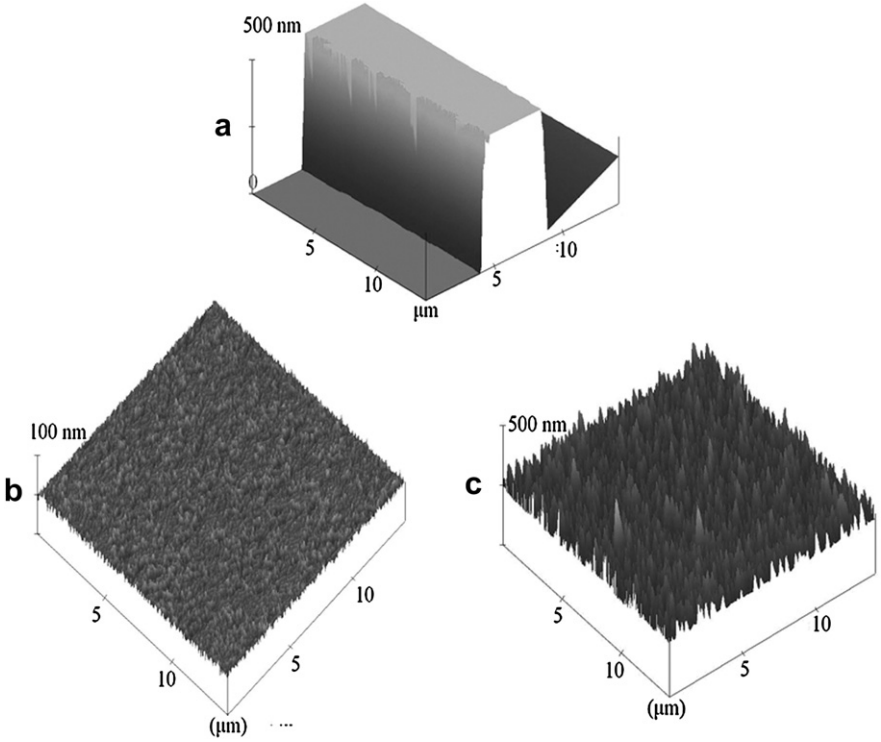

Fig. 8. AFM images of HBPI: (a) AFM 3D micrograph of the pattern, (b) surface roughness of the waveguide beam measured by AFM, (c) surface roughness of the silica layer of the substrate measured by AFM.

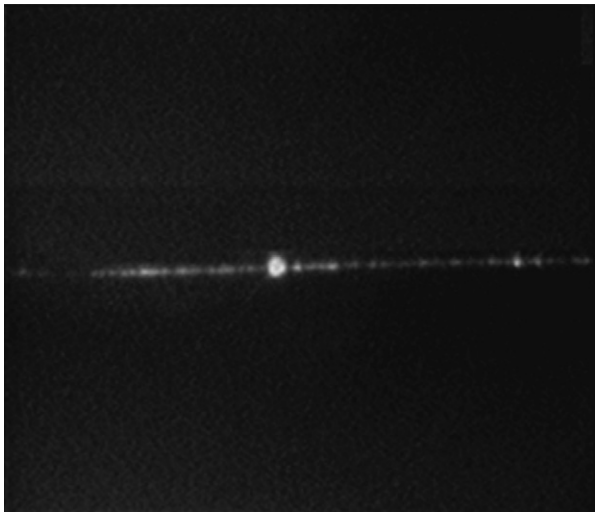

Fig. 9. Near-field pattern of a output-waveguide with TE polarized light at 1550 nm.

and 1.00–1.20 μm respectively. In addition, the –Cl and –CF_3-terminated polymers exhibit similar attenuation at the telecommunication wavelengths (1.31 and 1.55 μm) due to their similar harmonic (overtone) vibrational absorption [23–26]. These results show that the –Cl and –CF_3 shift the hydrogen–carbon overtone absorption to longer wavelength and reduced the optical loss at the telecommunication wavelengths. In addition, both Cl- and CF_3-terminaed polymers exhibit similar attenuation at telecommunication wavelengths due to the small second harmonic (overtone) vibrational absorption, which can avoid further increase in optical loss which bring by introducing C–H bonds.

RIs of the halogen-terminated HBPIs were measured by spectroscopic ellipsometer at 1.31 and 1.55 μm. The RI values are in the range of 1.5160–1.5309, 1.5807–1.6109 and 1.5863–1.5944 for HG-6F, HG-OD, and HG-BT series, respectively (Table 3). The HG-6F series with higher fluorine contents shows relatively lower RIs, because C–F bonds are much less polarizable than C–H bonds. HG-6F series showed relatively lower RIs because of their higher fluorine content. In fact, a good linear relationship is observed between RIs and –CF_3 contents as shown in Fig. 6. Taking the HG-OD series for example, RIs are increased from 1.5807 to 1.6109 as the feed ratio of 3,5-bis(trifluoromethyl)aniline is increased from 0 to 100%. This linear relationship represented good control of the RI by varying the feed ratio of terminal monomers. Compared with conventional copolymerization methods, the modification of the end groups by different halogen-containing monomers in HBPIs allows straightforward control of the RI values.

The in-plane/out-of-plane birefringences (Δn) measured for the halogen-terminated HBPIs at 650 nm are summarized in Table 3. The Δn values of the HG-6F series are as low as 0.003, which are lower than those of the linear polyimides [27]. Low birefringence can be attributed to the hyperbranched structures which effectively prevent dense molecular packing and prevent in-plane orientation of PI chains. Moreover, the –CF_3 groups and –O- linkages in the triamine monomer also lower the birefringence due to the added flexibility of the polymer chains.

3.3. Fabrication of polymer waveguide devices

Finally, several waveguide devices were fabricated using the HBPIs by RIE technique. Fig. 7 shows a typical SEM image of the core structure of straight (A) and flexural (B) waveguides fabricated with the polymer HG-6F ($2CF_3$ 100%). The typical ridge widths and heights of the waveguides are in the range of 1–5 μm. Fig. 8 shows the atomic force microscope (AFM) image of the polymer waveguide. In the 3D micrograph of the pattern, smooth surfaces are obtained for both of the top and sidewall of the core layer waveguide. Based on the AFM image, the film thickness was estimated as ca. 1 μm, and the surface roughness is less than 5 nm. The transmission spectra of the waveguide device were measured by a tunable laser at the center wavelength at 1550 nm and a spectrum analyzer. (Fig. 9) Light from a tunable semiconductor laser was coupled into the input-waveguide through a single-mode optical fiber. The near-field mode pattern at the output-channels was observed with a near-IR vidicon after magnification by an objective lens. The transmission spectra and near-field patterns demonstrate that the fluorinated HBPIs are a promising candidate for optical waveguide applications with low optical loss at the wavelengths for telecommunication.

4. Conclusions

A series of HBPIs with amino-, anhydride- and halogen-terminated end groups were prepared successfully. All the halogen-terminated HBPIs had excellent physical properties, including high glass transition temperatures, good thermal stabilities, and ease of film processing. By comparing NMR spectra of HBPIs with those of model compounds, DBs values of the amino- and anhydride-terminated HBPIs were found to be higher than 60% and 90%, respectively. Furthermore, the halogen-terminated HBPIs exhibited excellent optical properties. It was shown that high –CF_3 content could increase the film transparency, and the hyperbranched isotropic structures could reduce the birefringences. By substituting the large numbers of end groups with fluorinated and chlorinated monomers, the polymers may express precisely tunable RIs and ~~the~~ low optical loss at the same time. Consequently, ~~the~~ waveguide devices were successfully fabricated by RIE using the HBPIs, and these were found to exhibit low optical propagation losses at 1.55 μm.

Acknowledgment

The present work was supported by the National Natural Science Foundation of China (50773025).

References

[1] Fischbeck G, Moosburger R, Kostrzewa C, Achen A, Peermann K. Electron Lett 1997;33:518.
[2] Pitois C, Vukmirovic S, Hult A, Wiesmann D, Robertsson M. Macromolecules 1999;32:2903.
[3] Lee H-J, Lee M-H, Oh M-C, Ahn J-H, Han SG. J Polym Sci Part A Polym Chem 1999;37:2355.
[4] Smith DW, Babb DA. Macromolecules 1996;29:852.
[5] Matsuura T, Ishizawa M, Hasuda Y, Nishi S. Macromolecules 1992;25:3540.
[6] Badara C, Wang Z-Y. Macromolecules 2004;37:147.
[7] Kim E, Cho S-Y, Yeu D-M, Shin S-Y. Chem Mater 2005;17:962.
[8] Blythe AR, Vinson JR. Polym Adv Technol 2000;11:601.
[9] Chang C-C, Chen W-C. Chem Mater 2002;14:4242.
[10] Matsuura T, Yamada N, Nishi S, Hasuda Y. Macromolecules 1993;26:419.
[11] Matsuura T, Ando S, Sasaki S, Yamamoto F. Macromolecules 1994;27:6665.
[12] Hasegawa M, Horie K. Prog Polym Sci 2001;26:259.
[13] Kim Y-H. J Polym Sci Part A Polym Chem 1998;36:1685.
[14] Voit B. J Polym Sci Part A Polym Chem 2000;38:2505.
[15] Pitois C, Wiesmann D, Lindgren M, Hult A. Adv Mater 2001;13:1483.
[16] Fang J, Hidetoshi K, Ken-ichi O. Macromolecules 2000;33:4639.
[17] Fang J, Hidetoshi K, Ken-ichi O. J Memb Sci 2001; 182, 245.
[18] Chen H, Yin J. J Polym Sci Part A Polym Chem 2002;40:3804.
[19] Gao H, Wang D, Guan S-W, Jiang W, Jiang Z-H, Gao W-N, et al. Macromol Rapid Commun 2007;28:252.
[20] Hawker CJ, Fréchet JMJ. J Am Chem Soc 1991;113:4583.
[21] Holter D, Burgath A, Frey H. Acta Polym 1998;48:30.
[22] Kim YH, Beckerbauer R. Macromolecules 1968;1994:27.
[23] Ando S, Matsuura T, Sasaki S. Macromolecules 1992;25:5858.
[24] Qi Y-H, Ding J-F, Day M, Jiang J, Callender CL. Chem Mater 2005;17:676.
[25] Goodwin AA, Mercer FW, McKenzie MT. Macromolecules 1997;30:2767.
[26] Yen CT, Chen WC. Macromolecules 2003;36:3315.
[27] Han K, Lee HJ, Rhee H. J Appl Polym Sci 1999;74:107.